ELSEVIER

Biophysical Chemistry 124 (2006) 62–72

Biophysical Chemistry

http://www.elsevier.com/locate/biophyschem

# Pentacoordinate and hexacoordinate ferric hemes in acid medium: EPR, UV–Vis and CD studies of the giant extracellular hemoglobin of *Glossoscolex paulistus*

Leonardo Marmo Moreira [a], Alessandra Lima Poli [a], Antonio José Costa-Filho [b], Hidetake Imasato [a,*]

[a] *Instituto de Química de São Carlos, Universidade de São Paulo, CEP 13566-590, São Carlos, SP, Brazil*
[b] *Instituto de Física de São Carlos, Universidade de São Paulo, C.P. 369, CEP 13560-950, São Carlos, SP, Brazil*

Received 19 April 2006; received in revised form 30 May 2006; accepted 30 May 2006
Available online 6 June 2006

**Abstract**

The equilibrium complexity involving different axially coordinated hemes is peculiar to hemoglobins. The pH dependence of the spontaneous exchange of ligands in the extracellular hemoglobin from *Glossoscolex paulistus* was studied using UV–Vis, EPR, and CD spectroscopies. This protein has a complex oligomeric assembly with molecular weight of 3.1 MDa that presents an important cooperative effect. A complex coexistence of different species was observed in almost all pH values, except pH 7.0, where just aquomet species is present. Four new species were formed and coexist with the aquomethemoglobin upon acidification: (i) a "pure" low-spin hemichrome (Type II), also called hemichrome B, with an usual spin state $(d_{xy})^2(d_{xz},d_{yz})^3$; (ii) a strong $g_{max}$ hemichrome (Type I), also showing an usual spin state $(d_{xy})^2(d_{xz},d_{yz})^3$; (iii) a hemichrome with unusual spin state $(d_{xz},d_{yz})^4(d_{xy})^1$ (Type III); (iv) and a high-spin pentacoordinate species. CD measurements suggest that the mechanism of species formation could be related with an initial process of acid denaturation. However, it is worth mentioning that based on EPR the aquomet species remains even at acidic pH, indicating that the transitions are not complete. The "pure" low-spin hemichrome presents a parallel orientation of the imidazole ring planes but the strong $g_{max}$ hemichrome is a *HALS* (highly anisotropic low-spin) species indicating a reciprocally perpendicular orientation of the imidazole ring planes. The hemichromes and pentacoordinate formation mechanisms are discussed in detail.


*Keywords:* Hemoglobin; pH; Pentacoordinate; Hexacoordinate; Hemichrome

## 1. Introduction

Large extracellular hemoglobins have been employed as potential blood substitutes [1]. Strand et al. [2] have proposed that erythrocruorins are useful model systems for developing therapeutic blood substitutes due to their extracellular nature, large size and resistance to oxidation. Hirsch et al. [1] have suggested that the *Lumbricus terrestris* hemoglobin in the ferrous form, at neutral pH, exhibits similar oxygen affinity and cooperativity to that of human hemoglobin. Other advantages to use this hemoglobin class are its natural character and structural stability. It also shows low probability to promote immunogenic responses since cell membranes are not present and, unlike tetrameric hemoglobins, it does not undergo subunit dissociation upon dilution [3,4]. Recently, Vinogradov [5,6] argued that giant extracellular hemoglobins represent a summit of complexity for oxygen-binding heme protein.

In the present work, the behavior of the extracellular methemoglobin of the annelid *Glossoscolex paulistus* (HbGp) as a function of pH has been evaluated. This worm is prevalent in sites near the cities of Piracicaba, Araras and Rio Claro in the state of São Paulo, Brazil [7]. Its hemoglobin is a giant biopolymer that shows a molecular mass of 3.1 MDa [8] and a complex assembly with a hexagonal double-layered (HBL) oligomeric structure [9,10] that dissociates in alkaline and acid mediums [11,12]. This hemoprotein shows interesting features regarding natural selection, such as its adaptation in sulfide-rich environments [10,13].

* Corresponding author.
*E-mail address:* hidetake@iqsc.usp.br (H. Imasato).

0301-4622/$ - see front matter © 2006 Elsevier B.V. All rights reserved.
doi:10.1016/j.bpc.2006.05.030

*G. paulistus* hemoglobin belongs to the same class of hemoglobin as *L. terrestris*, which is one of the most studied hemoglobins [14–20], thus showing a highly cooperative oxygen binding process [14,21]. It consists of an arrangement of two heme-containing subunits (monomer and disulfide-bonded trimer T) with molecular mass in the range 15–19 kDa and non-globin linker subunits of 24 to 32 kDa [10,14]. Some studies suggest that the linker chains present not only structural functions but also superoxide dismutase activity [22]. A common model for the quaternary structure, so-called "bracelet model", has been employed to explain its assembly [14].

Many studies about equilibrium between different coordination states of hemoglobins have been developed. The equilibrium of heme proteins involves the coexistence of many species depending on medium conditions [23–25]. In fact, changing pH and ionic strength leads to modifications in the first coordination sphere. These induce alterations of the spin state, ligand orientation, and process of exchange of iron ligands. Furthermore, there are species with different number of coordination, i.e., the coexistence of hexacoordinate, pentacoordinate [24], and tetracoordinate [26,27] forms are possible. It has been described that below pH 4 some heme proteins, such as myoglobin and horseradish peroxidase, lose the sixth ligand, thus converting the heme prosthetic groups to water ligated pentacoordinate [28]. In fact, one of the most significant developments in porphyrin chemistry over the last 20 or so years has been the understanding of the extraordinary flexibility of the porphyrin ring [29], that is associated with heme environment, including axial ligands and spin state of the ferric ion. In heme proteins, asymmetric distortions of the porphyrin macrocycle are induced by axial ligands, asymmetric peripheral substituents, and the anisotropic protein environment [30].

In several recent reports, the hemichrome formation has been correlated to the biological function of tetrameric hemoglobins. On the one hand, Robinson et al. [31], studying the pH-dependent aquomet-to-hemichrome transition of horse methemoglobin in acid medium, have proposed that *in vivo* hemichrome formation is related to a more solvent-exposed heme group. The appearance of bis-histidine in both ferric and ferrous forms of neuroglobin and cytoglobin has also been explained by solvent channel formation [32,33].

The modification mechanism of the first coordination sphere is very relevant in the research of heme proteins. There is a strong correlation between the polypeptide assembly and the ligand properties of the ferric ion. Hence, the conformation changes of the polypeptidic chains can alter the ligands of the ferric center. For example, the pentacoordinate species formation can be associated with the first step of an unfolding process [26,27].

The presence of a pentacoordinate species can have a general significance to all native proteins, not only to myoglobins and hemoglobins [34]. Viola et al. [35], for example, suggest that cytochrome *c* shows an interplay between redox, structural, ligand binding, and recognition properties. In fact, various metalloporphyrin complexes are pentacoordinate, resembling to the pentacoordinate heme proteins [36,37].

The aim of the present work is to contribute in the understanding of the structure–activity relationship of heme proteins, specially of the *G. paulistus* giant hemoglobin, characterizing the species in the first coordination sphere of the iron as a function of pH. This work focuses on the transitions of the extracellular hemoglobin in the acidic medium. UV–Vis and electron paramagnetic resonance (EPR) were used to monitor modifications in the spin state as well as in the coordination environment at the metallic center, and circular dichroism (CD) to follow changes in the protein folding upon acidification.

## 2. Methods and materials

### 2.1. Protein preparation

The hemoglobin of *G. paulistus* was prepared using freshly drawn blood from worms. The blood sample was purified by ultra centrifugation and gel filtration in Sephadex G-200 column at pH 7.0 [11].

### 2.2. UV–Vis measurements

Electronic absorption spectra in the wavelength range of 250 to 700 nm were obtained as a function of pH, using a SHIMADZU UV-1601 PC spectrophotometer at room temperature. The absorbance of the samples at 415 nm was kept below 1.0 using a 1 cm path length cell, with concentration approximately 0.2 mg $ml^{-1}$ based on $\varepsilon_{415}$=3.7 ml $mg^{-1}$ $cm^{-1}$ at pH 7.0 [38].

### 2.3. EPR measurements

X-band (9.5 GHz) EPR spectra were measured on a Brucker Elexsys E580 spectrometer at 4 and 12 K. The temperature was controlled by an Oxford ITC 503 cryogenic system. EPR samples (50 μl) containing approximately 20 mg $ml^{-1}$ of the protein were frozen by immersion in liquid nitrogen and then placed in the spectrometer rectangular cavity. The microwave power was 4.0 mW and other acquisition conditions, such as modulation amplitude were adjusted to achieve optimal signal-to-noise ratio without signal distortion or saturation. All EPR data were corrected by subtracting a baseline corresponding to the EPR signal of the buffer.

### 2.4. CD measurements

CD spectra were obtained in a Jasco J715 (Jasco Co., Japan) as a function of pH employing the 0.2 cm path length cylindrical cell. Protein concentration was 0.22 mg $ml^{-1}$ based on $\varepsilon_{415}$=3.13 ml $mg^{-1}$ $cm^{-1}$ [39]. The residual ellipticity, [$\theta$] in mdegree $dmol^{-1}$ $cm^2$, was obtained using the amino acid residue average molecular mass of 117 g $mol^{-1}$.

## 3. Results and discussion

### 3.1. UV–Vis measurements

UV–Vis measurements at pH 7.0 resulted in typical spectrum of a single aquomet species. This species is found in

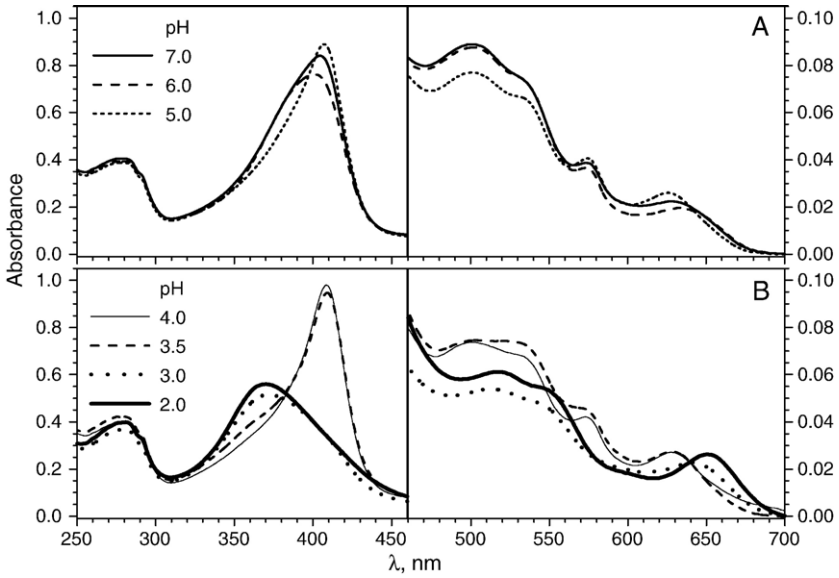


Fig. 1. Absorbance spectra of *Glossoscolex paulistus* hemoglobin. Conditions: 20 mM Tris–HCl buffer; GpHb concentration was 0.2 mg $ml^{-1}$. (A) pH 7.0, 6.0 and 5.0; (B) pH 4.0, 3.5, 3.0 and 2.0.

a great number of hemoglobins with similar bands [40–44] and is identified by a Soret band at 405 nm, a Q band at 500 nm and an LMCT band at 630 nm (Fig. 1).

The decrease in pH values from pH 6.0 to pH 3.0 causes an absorbance increase and a small red shift of the Soret band simultaneously, indicating the hemichrome formation, i.e., a bis-histidine complex formation, which is characterized by Q bands at 532 and 574 nm [44–47]. Therefore, this spectral change is associated with the distal histidine coordination to the ferric ion. The movement of the distal histidine imidazole towards the metal center is probably the result of a small change in the globin arrangement in the heme pocket.

A drastic spectral transition can be observed around pH 3.0. In fact, a Soret band blue shift relative to the pH 7.0 spectrum can be verified with a simultaneous decrease of absorbance, which indicate the formation of a pentacoordinate species as previously observed for several recent works [26,27,41–43,48–73].

Moreover, the pronounced Soret band shift to 371 nm occurs probably due to an initial unfolding process [42,43,59]. The very broad and asymmetric Soret band may be caused by the coexistence of two pentacoordinated species, i.e., a species with proximal histidine as fifth ligand and a pentacoordinated free hemin with water as fifth ligand [74].

Harris and Loew [75], using a semiempirical quantum chemical INDO/ROHF/CI method, calculated the electronic structure of cytochrome *P*450 in order to explain the optical spectra of the high- and low-spin states. The comparison of the calculated spectra of the two spin states reveals that, upon change of the Fe(III) from a low- to a high-spin state, a blue shift does indeed occur in the Soret band as observed for HbGp at pH lower than 3.5 (Fig. 1). They interpreted this shift as a direct result of the spin-state change. In the low-spin state, there is an enhanced mixing of the iron *d* orbital (*eg*) and porphyrin 4*eg* ($\pi*$) orbitals, which results in lower energy *eg* ($\pi^*$) states. This occurs because the higher ligand field of the low-spin state increases the energy of the *eg* orbitals, allowing higher interaction between these metallic orbitals and the porphyrin orbitals. Neya et al. [76] admitted to offer a similar explanation for myoglobins, i.e., the shorter wavelength would be associated with the high-spin state, while longer wavelength would be related to low-spin state.

The pentacoordinated species formation can also be confirmed by the analysis of the LMCT (Ligand-to-Metal Charge Transfer) band (Fig. 1). This band shows a red shift in the same pH range that causes the Soret band blue shift. Recent results showed that an LMCT band between 600 and 650 nm indicates a high-spin species [77,78]. Pentacoordinated high-spin hemes have been assigned to LMCT bands at 645 nm [50,59,61] or, at least, near to 645 nm [26,56, 62,79].

The UV–Vis data can be rationalized in terms of a mechanism for the transition upon acidification as follows. The stability of the aquomet species at pH 7.0 is provided by the presence of a water molecule in the nonpolar pocket, which is stabilized by binding to the heme iron [80]. Thus, the stability of the aquomet species can be explained mainly by two factors: the hydrophobicity of the heme pocket and the strong hydrogen bond between the water ligand and the distal histidine.

The aquomet–hemichrome transition must be due to the protonation of the nitrogen of the distal histidine, which decreases the ability of the histidine imidazole to stabilize the coordinated water molecule. Thus, the water molecule can easily dissociate from the first coordination sphere of the iron. Therefore, the absence of the hydrogen bond between the imidazole and the water molecule could be considered the initial step of the hemichrome formation [46,81].

The hemichrome–pentacoordinated transition can be originated by a competition between the ferric center and the protons for the imine-nitrogen of the imidazole. After imidazole protonation, the iron is shifted from the porphyrin nitrogen

plane towards the fifth ligand. The distal histidine is probably the displaced residue due to the higher tension of the distal coordination compared to the proximal site.

Besides that Boffi et al. reported that a strong σ-donor character of the fifth ligand decreases the coordination of other strong σ-donor in the sixth ligand position [74]. This fact occurs due to the weakening of the Fe–N bond of the sixth ligand by occupation of the $d_z^2$ antibonding orbital in the high-spin configuration, thus increasing electronic repulsion, and precluding a more intense superposition between the orbitals in the σ-bond [40]. Furthermore, the π-donor character of the imidazole to the $d^5$ metallic center is known in ferric porphyrin complexes and heme proteins [82] as well as in non-porphyrins complexes [83,84], such as tetraammineruthenium(III) complexes [85–87]. This *trans*-influence must increase the labilization caused by σ-bond. Therefore, the *trans*-influence caused by σ-bond as well as by π-bond must generate the loss of the sixth coordination, because these two ligations would be weaker, favoring the pentacoordinate species formation, which is a more stable species in these conditions. Corroborating this analysis, other works also confirm this π-donor ability of imidazole ligand [88,89] and other N-heterocyclic ligands [90].

This mechanism is similar to the one occurring *in vivo* during ferrous pentacoordinate formation, indicating a possible correlation between this process and the protein structure. In this way, the movement of the metallic center to the out-of-plane arrangement in the pentacoordinated species yields a *domed* conformation, which is very important to several functions of heme proteins [91].

### 3.2. EPR measurements

The EPR spectrum at pH 7.0 is characteristic of an axially symmetric high-spin species with $g_{//}$ and $g_{\perp}$ around 2.0 and 6.1, respectively (Fig. 2). In this case, only one component is observed, indicating the existence of one high-spin configuration assigned to the aquomet species. The acidification

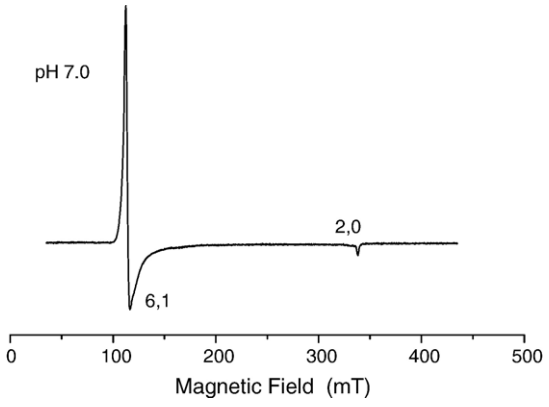


Fig. 2. Electron paramagnetic resonance spectrum of *Glossoscolex paulistus* hemoglobin with the *g*-values indicated. Conditions: 20 mM Tris–HCl buffer at pH 7.0 ($T$=4 K). EPR conditions: modulation amplitude, 0.1 mT; modulation frequency, 100 kHz; microwave power, 4.0 mW; microwave frequency, 9.4784 GHz.

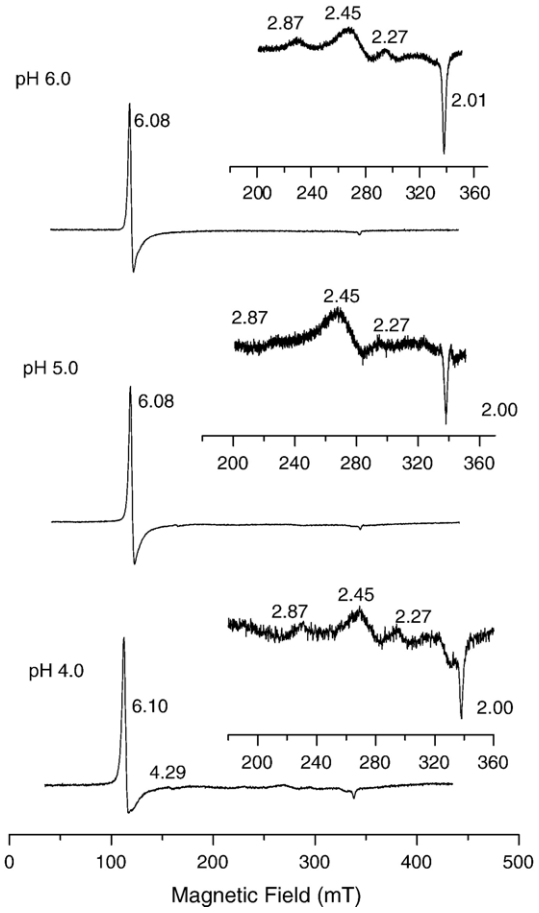


Fig. 3. Electron paramagnetic resonance spectra of *Glossoscolex paulistus* hemoglobin with the *g*-values indicated. Conditions: 20 mM Tris–HCl buffer; GpHb at pH 6.0 ($T$=4 K showing insert with $T$=12 K), GpHb at pH 5.0 ($T$=4 K showing insert with $T$=12 K), GpHb at pH 4.0 ($T$=4 K showing insert with $T$=12 K). EPR conditions: modulation amplitude, 0.1 mT; modulation frequency, 100 kHz; microwave power, 4.0 mW; microwave frequency, 9.4780 GHz.

causes the appearance of several species, whose spectra are shown in Figs. 3 and 4 as a function of the pH value. Overall, three low-spin species are formed in the spectra (see $g\sim2$ region of the spectrum—insert of Fig. 3), which are assigned to hemichromes, i.e., bis-histidine complexes. In hemoproteins, it is well established that bis-histidine hemes having two axial histidine ligands display similar EPR spectra with $g_z$ values between 2.9 and 3.6. The *g*-values of these complexes depend on the relative orientation of the two imidazole rings and on the orientation of these imidazoles with respect to the porphyrin plane [92,93]. These hemichromes show different electronic configurations: two of them are in the more usual spin state $(d_{xy})^2(d_{xz},d_{yz})^3$, and are characterized by *g*-values at 2.87 and 2.27 (Fig. 3) and by *g*-values around 3.47 (Fig. 4); the third hemichrome presents an unusual electronic configuration $(d_{xz},d_{yz})^4(d_{xy})^1$ with a resonance at 2.45 (Figs. 3 and 4). The $g$=4.3 line in Fig. 4 has been observed in other ferric proteins and it has been assigned to non-heme iron impurities [94,95]. Consequently, it will not be further considered in our discussion.

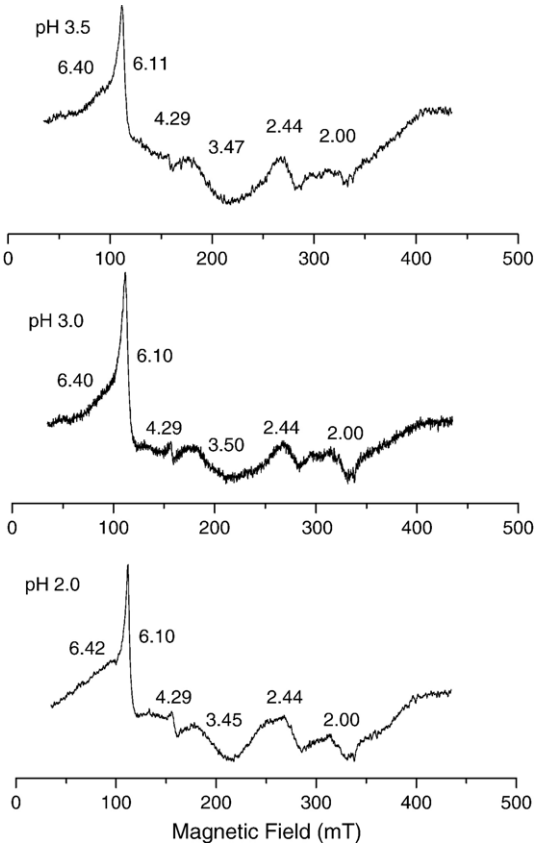


Fig. 4. Electron paramagnetic resonance spectra of *Glossoscolex paulistus* hemoglobin with the *g*-values indicated. Conditions: 20 mM Tris–HCl buffer. EPR conditions: $T=12$ K, modulation amplitude, 0.1 mT; modulation frequency, 100 kHz; microwave power, 4.0 mW; microwave frequency, 9.4794 GHz.

Between the hemichromes with more usual electronic configuration, the first species (*g*-values 2.87 and 2.27) presents mutually parallel imidazole ring orientation (Type II or B-hemichrome) [96], whereas in the second species (*g*-values around 3.47) those rings are in an orthogonal conformation [Type I hemichrome or *HALS* (highly anisotropic low-spin)] [96–103]. It is worth mentioning that the distinction of these hemichromes was possible only through EPR spectroscopy. The reason is the small difference of energy between these configurations [104,105]. In fact, Zaric et al. [104] investigated the factors determining conformations of imidazole axially coordinated to heme in heme proteins by analyzing 693 hemes in 432 different crystal structures of heme proteins from the Protein Data Bank (PDB). In this expressive collection, 65 were bis-histidine-ligated hemes and the authors explain that the energy balance between the two forms with usual spin state is the result of crystal field stabilization effects favoring the parallel form and steric effects that favor the perpendicular form. In heme model systems, the orientation of axial ligands can depend on crystal field stabilization effects or on steric effects caused by substituents on axial ligands and on the porphyrin. In heme proteins, the heme does not possess bulky substituents, but the protein environment can have a steric influence on the orientation of the axial ligands. Medakovic and Zaric [105] performed quantum chemical (DFT) calculations on heme model systems with non-substituted Fe-porphyrin core for the different orientations of the axially coordinated imidazoles. Their results indicate that perpendicular orientation (Type I hemichrome) can be explained by steric effects caused by propionic groups of porphyrin ring and by the histidine backbone.

McGarvey [106] has described a more detailed explanation for the HALS (Type I) hemichrome formation considering that imidazole planes, that were initially in a parallel arrangement, adopt a perpendicular configuration, which is similar to a tetragonal distortion. In this way, the heme avoids a classic Jahn-Teller effect, with the axial ligands preferring the perpendicular orientation, which shows smaller orbitals overlap with the iron orbitals than the parallel orientation, thus causing a smaller splitting of iron $d_\pi$ orbitals. Rieger [107] has reported that Type I hemichrome presents an apparent near-degeneracy of the $d_{xz}$ and $d_{yz}$ orbitals that is consistent with the crystal structure, which showed that the two ligands lie in perpendicular planes because of the similar orbitals overlap to $d_{xz}$ and $d_{yz}$.

The $g_\perp$-value of 2.45 suggests the unusual configuration $(d_{xz},d_{yz})^4(d_{xy})^1$ for the heme-iron [96,108,109], also called Type III hemichrome, that probably occurs because of a great influence of the globin, causing a large distortion of the porphyrin ring. Interactions between the protein backbone and the porphyrin may be responsible for the macrocycle distortions from planarity *in vivo* that could modulate their physical and chemical properties [109]. This porphyrin distortion modifies the superposition of the $d_\pi$ orbitals with the axial ligand orbitals, in such a way that the $d_{xy}$ orbitals become the HOMO. The $g_{//}$ of this spectrum is not observed, but it would be between the *g*-values of 0.9 and 1.95 [96]. In agreement with Walker [96], this species can be identified as a Type III hemichrome.

After further acidification, an unexpected signal with *g* greater than 3.2 [96,110] was observed (Fig. 4). Some authors have analyzed this signal in other hemoglobins and ferric complexes [77]. The so-called hemichrome with strong $g_{max}$ (Type I), i.e. $g>3.2$, is an approximately low-spin state ($S=1/2$), showing a smaller splitting of orbitals than the typical low-spin species as the Type II hemichrome [111,112]. Thus, in bis-coordinated systems with two strong-field ligands, such as imidazoles and most pyridines, the spin state is $S=1/2$, showing very different *g*-values when compared to complexes formed with weak axial ligands, which tends to form an intermediate spin state of $S=3/2$ [113,114]. In agreement with many works [100,101,115], the $g\sim3.5$ corresponds to the $g_z$-value and the other *g*-values for the same configuration were not observed.

As for the Type II hemichrome (*g*-values at 2.87 and 2.27), its electronic configuration is $(d_{xy})^2(d_{xz},d_{yz})^3$, and the third *g*-value obey the Griffith condition ($\sum g^2\sim16$) [116], yielding a *g*-value of 1.61. The higher proximity of these *g*-values indicates that this EPR spectrum has large rhombicity with axial ligand planes aligned almost parallel to the $N_p$–Fe–$N_p$ direction, where $N_p$ are the diametrically opposed pyrrole-

nitrogens in the porphyrin ring [96,111]. Unfortunately, it is not possible to perform a similar analysis for the Type I hemichrome (HALS) because only one component of *g*-tensor was experimentally determined.

In complexes with a parallel orientation of two planar axial ligands, such as Type II hemichromes, the porphyrin remains planar [97,117], whereas the porphyrin ring is almost invariably distorted from planarity in porphyrin complexes with two planar axial ligands in a perpendicular orientation [96,104,105]. The *d*-orbital splittings are very important to the reactivity of the ferric center of the hemichromes. The perpendicular alignment of planar axial ligands could lead to a positive shift in reduction potential of up to 50 mV over that observed for parallel alignment, all other structural and environmental factors being equal [96,111,118].

Besides the hemichromes discussed above, pentacoordinated species are also identified by the EPR spectra at pH lower than 3.5 (Fig. 4). The hemichrome–pentacoordinated transition is characterized by an increase of the rhombic features observed by the high-spin signal (*g*-value around 6.0). In fact, the broadening of the spectral line in $g \cong 6.4$ indicates a second spectral component (Fig. 4). This new spectral component suggests the presence of a pentacoordinate species, corroborating the UV–Vis measurements. Usually, a pentacoordinate system has lower symmetry than a hexacoordinate system. Furthermore, this asymmetry is increased by the *domed* conformation, i.e., the out-of-plane arrangement of the metallic center [91].

A correlation between histidine orientation and degree of the ferric ion displacement from the heme plane with the length of the histidine–iron bond has been reported [31]. The occurrence of an intense resonance at $g \cong 3.5$ and an increase of asymmetry in the axial line $g \cong 6.4$ at pH 3.5 (Fig. 4) allowed the inference that the formation of the strong $g_{max}$ (Type I) hemichrome is somehow related to the appearance of the pentacoordinate species (Fig. 4A). Hence, the strong $g_{max}$ hemichrome formation could be a prerequisite to formation of the pentacoordinated species. The strong $g_{max}$ (Type I) hemichrome represents a weakening of the axial histidines coordination as compared to the low-spin Type II hemichrome. Nistor et al. [95] have found similar transition in acidic medium to a neuroglobin ferric, suggesting that histidine disruption from hemichrome is a mechanism to generate pentacoordinate species.

Blumberg and Peisach associate the spin transition to yield hemichrome as a consequence of disruption of hydrophobic interactions [47]. In agreement with Tsuka [119], the cooperative breaking of van der Waals contacts between the porphyrin and the globin would be associated with the spin state change. It is possible that the aquomet–hemichrome–pentacoordinate transition could indicate a gradual increase of solvent accessibility allowed by an initial unfolding, corroborating previous studies on whole hemoglobin of *G. paulistus* [39]. Indeed, Imasato et al. [11] characterized the acid dissociation of the whole hemoglobin of *G. paulistus* by resonant light scattering (RLS) in pH values below 5.0. This dissociation of oligomeric fractions must enhance the contact of the water solvent molecules with the ferric center, becoming more pronounced the mechanism of transition between species, specially the pentacoordinate species formation, which occurs in pH < 5.0.

The EPR results suggest that there is a sequence of species formation as function of pH, which is probably associated to activity–structure relationship of this hemoglobin (Scheme 1).

The EPR spectra indicate that aquometHb remains even in the highly acid pH. The coexistence of various species is a characteristic property of most hemoglobins, which makes the complex equilibrium of this supramolecular system.

### 3.3. CD measurements

Far-UV circular dichroism spectra for the HbGp as a function of pH are shown in Fig. 5. At pH 7.0, the CD spectrum is characterized by positive bands at 195, and two negative bands at 208 and 222 nm assigned to a considerable α-helix content as expected in hemoglobins. Upon acidification at pH < 5, a decrease of both 195 nm and 222 nm bands is observed and it is associated with a decrease of helical content. The stability of the aquomet species at pH 7.0 (observed as a single-component in the EPR spectrum of Fig. 2) is due to the hydrophobicity of the heme pocket. Decreases in pH lead to an increase of the solvent accessibility, destabilizing the aquomet species. This process is probably related mainly to loss of helical content.

The absolute values of residual ellipticity at 195 and 222 nm increase gradually from pH 2.0 up to pH 4.0. This behavior is somehow disturbed at pH greater than 5.0, and the bands get to a

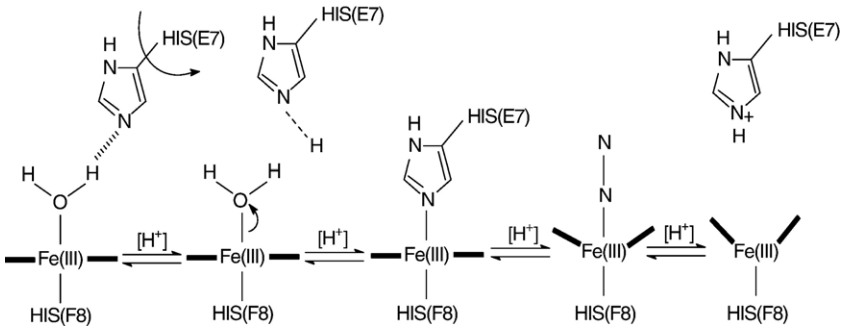


Scheme 1. The broad lines represent the side view of heme surfaces and the fourth model indicates the change of orientation of the distal histidine in relation to the heme, i.e., the side view of the distal histidine coordinated to the ferric center constituting the hemichrome HALS.

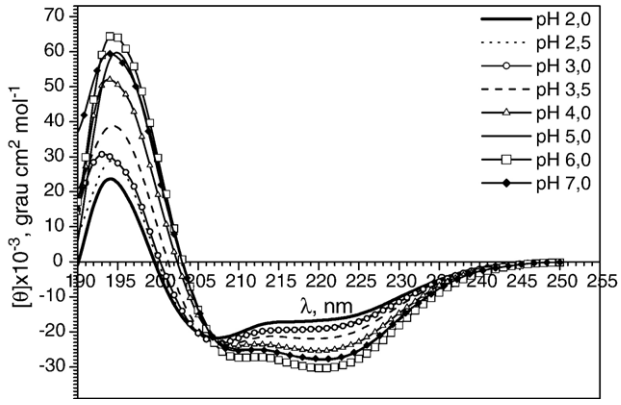


Fig. 5. CD spectra of *Glossoscolex paulistus* hemoglobin as function of pH. Conditions: protein concentration was 0.22 mg $ml^{-1}$ ($\varepsilon_{415}$=3.13 ml $mg^{-1}$ $cm^{-1}$).

maximum around pH 6.0. Such an effect can be due to the proximity between pH 6.0 and the protein isoelectric point (pI). The pI for this class of hemoglobins is acid [5] like, for example, the pI for the *L. terrestris* hemoglobin that is 5.5 [120]. This spectral behavior could be associated with the "aggregation" state of the hemoglobin that is maximum at the pI because of minimum electrostatic repulsion [121]. In pH lower than pI the loss of α-helix is drastic, indicating significant influence of the acid medium on the globin.

The relationship between the increase of solvent accessibility in the heme pocket and the loss of secondary structure would indicate that the formation of the pentacoordinate species could be an initial step of the denaturation process. Madura et al. [21] have reported that, in most vertebrate hemoglobins, changes in protein tertiary structure are induced by either ligand binding or changes in oligomeric assembly at the heme neighborhood. Nevertheless no such changes are observed for *L. terrestris* hemoglobin. Considering the similarity between *L. terrestris* and *G. paulistus* hemoglobins, it is possible to infer that the subunit assembly of a giant extracellular hemoglobin is less susceptible to the solvent permeability than vertebrate hemoglobins. Hundahl et al. [122] assert that the small effects of water in the extracellular invertebrate hemoglobins may be correlated with small surface-to-volume ratios in these high-molecular-weight proteins that pose a limit to water-accessible sites, and suggest smaller quaternary structural changes when compared to dimeric and tetrameric hemoglobins. Other studies are in progress in order to analyze the implication of the pentacoordinate formation in the acid denaturation.

## 4. Conclusions

The giant extracellular hemoglobin of *G. paulistus* was studied in the acidic pH range. The coexistence of five species was observed: aquomethemoglobin, strong $g_{max}$ or HALS hemichrome (Type I), low-spin hemichrome (Type II), hemichrome with an unusual spin state $(d_{xz},d_{yz})^4(d_{xy})^1$ (Type III) and a high-spin pentacoordinate species with a spin state ($d_{xz}$, $d_{yz})^2(d_{xz})^1(d^2_{x-y}{}^2)^1(d^2_z)^1$.

The hemichrome and pentacoordinate formation are explained by protonation of the histidines associated with the increase of the water accessibility to the heme pocket and the smaller possibility for hydrogen bond formation. The influence of the hydrogen bond in the stability of the sixth ligand is decisive to the consequent heme properties, such as electronic structure, ligand affinities, coordination number, redox potential and macrocycle conformations [73,121,123–127]. Furthermore, this greater accessibility could be related to the subunit dissociation, in a similar way to the alkaline process, where *d* monomer dissociates from the trimer, at pH 9.0. Finally, the presence of the pentacoordinate could be associated to an initial acid denaturation mechanism.

It is likely that the transition from the pure low-spin hemichrome to the *strong* $g_{max}$ hemichrome would be a prerequisite to the formation of the pentacoordinate species. This transition is due to an orientational change of the axial ligands, which represent a weakening of the histidine–metal ligation.

## Acknowledgments

The authors are indebted to Professor M. Tabak for helpful suggestions and to the Andressa P. A. Pinto for CD measurements. The authors are also grateful to CNPq for the student grant to L. M. Moreira. AJCF would like to thank CNPq and PRONEX/FAPESP/CNPq (Grant No. 03/09859-2).

## References

[1] R.E. Hirsch, L.A. Jelicks, B.A. Wittenberg, D.K. Kaul, H.L. Shear, J.P. Harrington, A first evaluation of the natural high molecular weight polymeric *Lumbricus terrestris* hemoglobin as an oxygen carrier, Artif. Cells Blood Substit. Immobil. Biotechnol. 25 (1997) 429–444.

[2] K. Strand, J.E. Knapp, B. Bhyravbhatia, W.E. Royer Jr., Crystal structure of the hemoglobin dodecamer from *Lumbricus* erythrocruorin: allosteric core of giant annelid respiratory complexes, J. Mol. Biol. 344 (2004) 119–134.

[3] S.C. Dorman, J.P. Harrington, M.S. Martin, T.V. Johnson, Determination of the formal reduction potential of *Lumbricus terrestris* hemoglobin using thin layer spectroelectrochemistry, J. Inorg. Biochem. 98 (2004) 185–188.

[4] J.L. Silva, M. Villas-Boas, C.F.S. Bonafe, N.C. Meirelles, Anomalous pressure dissociation of large protein aggregates, J. Biol. Chem. 264 (1989) 15863–15868.

[5] S.N. Vinogradov, The stoichiometry of the four linker subunits of *Lumbricus terrestris* hemoglobin suggests an asymmetric distribution, Micron 35 (2004) 127–129.

[6] A.R. Kuchumov, J.C. Taveau, J.N. Lamy, J.S. Wall, R.E. Weber, S.N. Vinogradov, The role of linkers in the reassembly of the 3.6 MDa hexagonal bilayer hemoglobin from *Lumbricus terrestris*, J. Mol. Biol. 289 (1998) 1361–1374.

[7] G. Righi, Topography of circulatory system of *Glossoscolex paulistus* Michaelsen 1926 (Oligochaeta, Glossoscolecidae), Monit. Zool. Ital. 6 (1972) 19–36.

[8] M.C.P. Costa, C.F.S. Bonafé, N.C. Meirelles, F. Galembeck, Sedimentation coefficient and minimum molecular-weight of extracellular hemoglobin of *Glossoscolex paulistus* Oligochaeta, Br. J. Med. Res. 21 (1988) 115–118.

[9] N.C. Meirelles, B. Oliveira, E. de Paula, S. Marangoni, G.M. Rennebeck, Erythrocruorin of *Glossoscolex paulistus* (*Oligochaeta*, *Glossocolecidae*)—dissociation at alkaline pH and its ligand properties as revealed by chemical, immunochemical and electron microscopy studies, Comp. Biochem. Physiol. 88A (1987) 337–379.

[10] F. Zal, B.N. Green, P. Martineau, F.H. Lallier, A. Toulmond, S.N. Vinogradov, J.J. Childress, Polypeptide chain composition diversity of hexagonal-bilayer haemoglobins within a single family of annelids, the Alvinellidae, Eur. J. Biochem. 267 (2000) 5227–5236.
[11] H. Imasato, M.H. Tinto, J.R. Perussi, M. Tabak, Fluorescence studies of extracellular hemoglobin of *Glossoscolex paulistus* obtained by gel filtration, Comp. Biochem. Physiol. 112B (1995) 217–226.
[12] A.L. Poli, L.M. Moreira, A.A. Hidalgo, H. Imasato, Autoxidation studies of extracellular hemoglobin of *Glossoscolex paulistus* at pH 9: cyanide and hydroxyl effect, Biophys. Chemist. 114 (2005) 253–260.
[13] X. Bailly, S. Vinogradov, The sulfide binding function of annelid hemoglobins: relic of an old biosystem? J. Inorg. Biochem. 99 (2005) 142–150.
[14] A. Krebs, P. Zipper, S.N. Vinogradov, Lack of size and shape alteration of oxygenated and deoxygenated *Lumbricus terrestris* hemoglobin? Biochim. Biophys. Acta 1297 (1996) 115–118.
[15] P.D. Martin, A.R. Kuchumov, B.R. Green, R.W.A. Oliver, E.H. Braswell, J.S. Wall, S.N. Vinogradov, Mass spectrometric composition and molecular mass of *Lumbricus terrestris* hemoglobin: a refined model of its quaternary structure, J. Mol. Biol. 255 (1996) 154–169.
[16] E. Viana, C.H.T.P. Silva, M. Tabak, H. Imasato, R.C. Garrat, A molecular model for the d chain of the giant haemoglobin from *Lumbricus terrestris* and its implications for subunit assembly, Biochim. Biophys. Acta 1383 (1998) 130–142.
[17] F. Haas, A. Kuchumov, J.C. Taveau, N. Boisset, S.N. Vinogradov, J.N. Lamy, Three-dimensional reconstruction of native and reassembled *Lumbricus terrestris* extracellular hemoglobin. Localization of the monomeric globin chains, Biochemistry 36 (1997) 7330–7338.
[18] F. Mouche, N. Boisset, P.A. Penczek, *Lumbricus terrestris* hemoglobin —the architecture of linker chains and structural variation of the central toroid, J. Struct. Biol. 133 (2001) 176–192.
[19] E. Daniel, A. Lustig, M.M. David, Y. Tsfadia, On the molecular mass of *Lumbricus* erythrocruorin, Micron 35 (2004) 131–132.
[20] O.H. Kapp, G. Polidori, M.G. Mainwaring, A.V. Crewe, S.N. Vinogradov, The reassociation of *Lumbricus terrestris* hemoglobin dissociated at alkaline pH*, J. Biol. Chem. 259 (1984) 628–639.
[21] J.D. Madura, E.A. Salter, A. Wierzbicki, P. Danal, J.P. Harrington, Homology models for the tetrameric and dodecameric complexes of *Lumbricus terrestris* hemoglobin, J. Mol. Struct. 592 (2002) 173–181.
[22] S.I. Liochev, A.R. Kuchumov, S.N. Vinogradov, I. Fridovich, Superoxide dismutase activity in the giant hemoglobin of the earthworm, *Lumbricus terrestris*, Arch. Biochem. Biophys. 330 (1996) 281–284.
[23] D. Morikis, P.M. Champion, B.A. Springer, S.G. Sligar, Resonance Raman investigations of site-directed mutants of myoglobin: effects of distal histidine replacement, Biochemistry 28 (1989) 4791–4800.
[24] S. Dasgupta, D.L. Rousseau, H. Anni, T. Yonetani, Structural characterization of cytochrome *c* peroxidase by resonance Raman scattering, J. Biol. Chem. 264 (1989) 654–662.
[25] E. Wajnberg, G. Bemski, J. El-Jaick, O.C. Alves, Nitrosyl hemoglobins: EPR above 80 K, Int. J. Biol. Macromol. 18 (1996) 231–235.
[26] J.T. Sage, D. Morikis, P.M. Champion, Spectroscopic studies of myoglobin at low pH: heme structure and ligation, Biochemistry 30 (1991) 1227–1237.
[27] V. Palaniappan, D.F. Bocian, Acid-induced transformations of myoglobin. Characterization of a new equilibrium heme-pocket intermediate, Biochemistry 33 (1994) 14264–14274.
[28] J. Cheek, D.W. Low, H.B. Gray, J.H. Dawson, Histidine-tailed microperoxidase-10: a pH-dependent ligand switch, Biochem. Biophys. Res. Commun. 253 (1998) 195–198.
[29] H.M. Marques, KL. Brown, Molecular mechanics and molecular dynamics simulations of porphyrins, metalloporphyrins, heme proteins and cobalt corrinoids, Coord. Chem. Rev. 225 (2002) 123–158.
[30] R. Schweitzer-Stenner, D. Bigman, Electronic and vibronic contributions to the band splitting in optical spectra of heme proteins, J. Phys. Chem., B 105 (2001) 7064–7073.
[31] V.L. Robinson, B.B. Smith, A. Arnone, A pH-dependent aquomet-to-hemichrome transition in crystalline horse methemoglobin, Biochemistry 42 (2003) 10113–10125.
[32] H. Sugimoto, M. Makino, H. Sawai, N. Kawada, K. Yoshizato, Y. Shiro, Structural basis of human cytoglobin for ligand binding, J. Mol. Biol. 339 (2004) 873–885.
[33] A. Pesce, S. Dewilde, M. Nardini, L. Moens, P. Ascenzi, T. Hankeln, T. Burmester, M. Bolognesi, The human brain hexacoordinated neuroglobin three-dimensional structure, Micron 35 (2004) 63–65.
[34] T.K. Das, A. Boffi, E. Chiancone, D.L. Rousseau, Hydroxide rather than histidine is coordinated to the heme in five-coordinate ferric *Scapharca inaequivalvis* hemoglobin, J. Biol. Chem. 274 (1999) 2916–2919.
[35] F. Viola, S. Aime, M. Coletta, A. Desideri, M. Fasano, S. Paoletti, C. Tarricone, P. Ascenzi, Azide, cyanide, fluoride, imidazole and pyridine binding to ferric and ferrous native horse heart cytochrome *c* and to its carboxymethylated derivative: a comparative study, J. Inorg. Biochem. 62 (1996) 213–222.
[36] P. Turner, M.J. Gunter, Carbon-13 NMR spectroscopy, electron spin distributions, and valence state of pentacoordinate manganese tetraphenylporphyrin complexes, Inorg. Chem. 33 (1994) 1406–1415.
[37] J.A. González, L.J. Wilson, Spin-state isomerism in crystalline $[Fe^{III}(TPP)(OSO_2CF_3)]$, Inorg. Chem. 33 (1994) 1543–1553.
[38] S.C.M. Agustinho, M.H. Tinto, J.R. Perussi, M. Tabak, H. Imasato, Fluorescence studies of extracellular hemoglobin of *Glossoscolex paulistus* in met form obtained by sephadex gel filtration, Comp. Biochem. Physiol. 118A (1997) 171–181.
[39] S.C.M. Agustinho, M.H. Tinto, H. Imasato, T.T. Tominaga, J.R. Perussi, M. Tabak, Spectroscopy studies of the met form of the extracellular hemoglobin from *Glossoscolex paulistus*, Biochim. Biophys. Acta 1298 (1996) 148–158.
[40] M.F. Perutz, J.K.M. Sanders, D.H. Chenery, R.W. Noble, R.R. Pennelly, L.W.M. Fung, C. Ho, I. Giannini, D. Pörschke, H. Winkler, Interactions between the quaternary structure of the globin and the spin state of the heme in ferric mixed spin derivatives of hemoglobin, Biochemistry 17 (1978) 3640–3651.
[41] M.L. Quillin, R.M. Arduini, J.S. Olson, G.N. Phillips Jr., High-resolution crystal structures of distal histidine mutants of sperm whale myoglobin, J. Mol. Biol. 234 (1993) 140–155.
[42] S. Kamimura, A. Matsuoka, K. Imai, K. Shikama, The swinging movement of the distal histidine residue and autoxidation reaction for midge larval hemoglobins, Eur. J. Biochem. 270 (2003) 1433–1474.
[43] M.A. Gilles-Gonzalez, G. Gonzalez, M.F. Perutz, L. Kiger, M.C. Marden, C. Poyart, Heme-based sensors, exemplified by the kinase FixL, are a new class of heme protein with distinctive ligand binding and autoxidation, Biochemistry 33 (1994) 8067–8073.
[44] L. Vitagliano, G. Bonomi, A. Riccio, G.D. Prisco, G. Smulevich, L. Mazzarella, The oxidation process of Antarctic fish hemoglobins, Eur. J. Biochem. 271 (2001) 1651–1659.
[45] E.A. Rachmilewitz, J. Peisach, W.E. Blumberg, Studies on the stability of oxyhemoglobin A and its constituted chains and their derivatives, J. Biol. Chem. 246 (1971) 3356–3366.
[46] M. Tsuruga, A. Matsuoka, A. Hachimori, Y. Sugawara, K. Shikama, The molecular mechanism of autoxidation for human oxyhemoglobin. Tilting of the distal histidine causes nonequivalent oxidation in the β chains, J. Biol. Chem. 273 (1998) 8607–8615.
[47] C.P. Baron, L.H. Skibsted, H.J. Andersen, Peroxidation of linoleate at physiological pH: hemichrome formation by substrate binding protects against metmyoglobin activation by hydrogen peroxide, Free Radic. Biol. Med. 28 (2000) 549–558.
[48] T. Tada, Y. Watanabe, A. Matsuoka, M. Ikeda-Saito, K. Imai, Y. Nihei, K. Shikam, African elephant myoglobin with an unusual autoxidation behavior: comparison with the H64Q mutant of sperm whale myoglobin, Biochim. Biophys. Acta 1387 (1998) 165–176.
[49] A. Matsuoka, N. Kobayashi, K. Shikama, The Soret magnetic circular dichroism of ferric high-spin myoglobins, Eur. J. Biochem. 210 (1992) 337–341.
[50] J.A. Sigman, A.E. Pond, J.H. Dawson, Y. Lu, Engineering cytochrome *c* peroxidase into cytochrome *P*450: a proximal effect on heme-thiolate ligation, Biochemistry 38 (1999) 11122–11129.
[51] K. Rajarathnam, G.N. La Mar, M.L. Chiu, S.G. Sligar, J.P. Singh, K.M. Smith, $^1$H NMR hyperfine shift pattern as a probe for ligation state in

high-spin ferric hemoproteins: water binding in metmyoglobin mutants, J. Am. Chem. Soc. 113 (1991) 7886–7892.
[52] D. Morikis, P.M. Champion, B.A. Springer, K.D. Egeberg, S.G. Sligar, Resonance Raman studies of iron spin and axial coordination in distal pocket mutants of ferric myoglobin, J. Biol. Chem. 265 (1990) 12143–12145.
[53] J. Bujons, A. Dikiy, J.C. Ferrer, L. Banci, A.G. Mauk, Charge reversal of a critical active-site residue of cytochrome-*c* peroxidase characterization of the Arg48→Glu variant, Eur. J. Biochem. 243 (1997) 72–84.
[54] G. Smulevich, M. Paoli, G. De Sanctis, A.R. Mantini, F. Ascoli, M. Coletta, Spectroscopic evidence for a conformational transition in horseradish peroxidase at very low pH, Biochemistry 36 (1997) 640–649.
[55] P.J. Wright, A.N. English, Buffer-anion-dependent $Ca^{2+}$ leaching from horseradish peroxidase at low pH, J. Biol. Inorg. Chem. 6 (2001) 348–358.
[56] N. Kamiya, Y. Shiro, T. Iwata, T. Iizuka, H. Iwasaki, Heme environmental structure of a novel artificial myoglobin with closed heme pocket: site-specific chemical modification producing distal *N*-tetrazolylhistidine E7 by cyanogen bromide and azide ion, J. Am. Chem. Soc. 113 (1991) 1826–1829.
[57] C. Indiani, A. Feis, B.D. Howes, M.P. Marzocchi, G. Smulevich, Benzohydroxamic acid-peroxidase complexes: spectroscopic characterization of a novel heme spin species, J. Am. Chem. Soc. 122 (2000) 7368–7376.
[58] T. Tomita, G. Gonzalez, A.L. Chang, M. Ikeda-Saito, M. Gilles-Gonzalez, A comparative resonance Raman analysis of heme-binding PAS domains: heme iron coordination structures of the *Bj*FixL, *Ax*PDEA1, *Ec*Dos, and *Mt*Dos proteins, Biochemistry 41 (2002) 4819–4826.
[59] A. Ilari, A. Bonamore, A. Farina, K.A. Johnson, A. Boffi, The X-ray structure of ferric *Escherichia coli* Flavohemoglobin reveals an unexpected geometry of the distal heme pocket, J. Biol. Chem. 277 (2002) 23725–23732.
[60] A. Matsuoka, Y. Ohie, K. Imai, K. Shikama, The dimer–monomer conversion of *Cerithidea* Myoglobin coupled with the heme iron oxidation, Comp. Biochem. Physiol. 115B (1996) 483–492.
[61] P. D´Angelo, D. Lucarelli, S. della Longa, M. Benfatto, J.L. Hazemann, A. Feis, G. Smulevich, A. Ilari, A. Bonamore, A. Boffi, Unusual heme iron-lipid acyl chain coordination in *Escherichia coli* Flavohemoglobin, Biophys. J. 66 (2004) 3882–3892.
[62] Y. Yamamoto, K. Koshikawa, N. Terui, H. Mita, A. Matsuoka, K. Shikama, $^1$H-NMR study of dynamics and thermodynamics of $Cl^-$ binding to ferric hemoglobin of a midge larva (*Tokunagayusurika akamusi*), Biochim. Biophys. Acta. 1652 (2003) 136–143.
[63] L. Kiger, V. Baudin, A. Desbois, J. Pagnier, J. Kister, N. Griffon, Y. Henry, C. Poyart, M.C. Marden, Recombinant [Pheβ63]hemoglobin shows rapid oxidation of the β chains and low-affinity, non-cooperative oxygen binding to the α subunits, Eur. J. Biochem. 243 (1997) 365–373.
[64] N.S. Reading, S.D. Aust, Effect of modified hemes on the spectral properties and activity of manganese peroxidase, Arch. Biochem. Biophys. 359 (1998) 291–296.
[65] P. Visca, G. Fabozzi, A. Petrucca, C. Ciaccio, M. Coletta, G. De Sanctis, M. Bolognesi, M. Milani, P. Ascenzi, The truncated hemoglobin from *Mycobacterium leprae*, Biochem. Biophys. Res. Commun. 294 (2002) 1064–1070.
[66] S. Ojha, J. Hwang, Ö. Kabil, J.E. Penner-Hahn, R. Banerjee, Characterization of the heme in human cystathionine β-synthase by X-ray absorption and electron paramagnetic resonance spectroscopies, Biochemistry 39 (2000) 10542–10547.
[67] M.L. Estevam, O.R. Nascimento, M.S. Baptista, P. Di Mascio, F.M. Prado, A. Faljoni-Alario, M.R. Zucchi, I.S. Nantes, Changes in the spin state and reactivity of cytochrome *c* induced by photochemically generated singlet oxygen and free radicals, J. Biol. Chem. 279 (2004) 39214–39222.
[68] I.L. Nantes, M.R. Zucchi, O.R. Nascimento, A. Faljoni-Alario, Effect of heme iron valence state on the conformation of cytochrome *c* and its association with membrane interfaces, J. Biol. Chem. 276 (2001) 153–158.
[69] I.L. Nantes, A. Faljoni-Alario, O.R. Nascimento, B. Brandy, R. Gatti, E.J.H. Bechara, Modifications in heme iron of free and vesicle bound cytochrome *c* by *TERT*-butyl hydroperoxide: a magnetic circular dichroism and electron paramagnetic resonance investigation, Free Radic. Biol. Med. 28 (2000) 786–796.
[70] I.L. Nantes, A. Faljoni-Alario, A.E. Vercesi, K.E. Santos, E.J.H. Bechara, Liposome effect on the cytochrome *c*-catalyzed peroxidation of carbonyl substrates to triplet species, Free Radic. Biol. Med. 25 (1998) 546–553.
[71] S.C.M. Gandini, V.E. Yushmanov, M. Tabak, Interaction of Fe(III)- and Zn(II)-tetra(4-sulfonatophenyl) porphyrins with ionic and nonionic surfactants: aggregation and binding, J. Inorg. Biochem. 85 (2001) 263–277.
[72] E. Psylinakis, E.M. Davoras, N. Ioannidis, M. Trikeriotis, V. Petrouleas, D.F. Ghanotakis, Isolation and spectroscopic characterization of a recombinant bell pepper hydroperoxide lyase, Biochim. Biophys. Acta 1533 (2001) 119–127.
[73] Y. Shiro, I. Morishima, Modification of the heme distal side in myoglobin by cyanogen bromide. Heme environmental structures and ligand binding properties of the modified myoglobin, Biochemistry 23 (1984) 4879–4884.
[74] A. Boffi, T.K. Das, S.D. Longa, C. Spagnuolo, D.L. Rousseau, Pentacoordinate hemin derivatives in sodium dodecyl sulfate micelles: model systems for the assignment of the fifth ligand in ferric, Biophys. J. 77 (1999) 1143–1149.
[75] D. Harris, G. Loew, Mechanistic origin of the correlation between spin state and spectra of model cytochrome *P*450 ferric heme proteins, J. Am. Chem. Soc. 115 (1993) 5799–5802.
[76] S. Neya, M. Tsubaki, H. Hori, T. Yonetani, N. Funasaki, Unusual spin state equilibrium of azide metmyoglobin induced by ferric corrphycene, Inorg. Chem. 40 (2001) 1220–1225.
[77] T.A. Clarke, V. Dennison, H.E. Seward, B. Burlat, J.A. Cole, A.M. Hemmings, D.J. Richardson, Purification and spectropotentiometric characterization of *Escherichia coli* NrfB, a decaheme homodimer that transfers electrons to the decaheme periplasmic nitrite reductase complex, J. Biol. Chem. 279 (2004) 41333–41339.
[78] A. Boffi, L. Guarrera, L. Giangiacomo, C. Spagnuolo, E. Chiancone, Proximal and distal effects on the coordination chemistry of ferric *Scapharca* homodimeric hemoglobin as revealed by heme pocket mutants, Biochemistry 39 (2000) 3500–3504.
[79] G. Kobayashi, T. Nakamura, H. Ohmachi, A. Matsuoka, T. Ochiai, K. Shikama, Yeast flavohemoglobin from *Cândida norvegensis*, J. Biol. Chem. 277 (2002) 42540–42548.
[80] M.P. Roach, A.E. Pond, M.R. Thomas, S.G. Boxer, J.H. Dawson, The role of the distal and proximal protein environments in controlling the ferric spin state and in stabilizing thiolate ligation in heme systems: thiolate adducts of the myoglobin H93G cavity mutant, J. Am. Chem. Soc. 121 (1999) 12088–12093.
[81] G.M. Giacometti, E. Antonini, M. Brunori, Kinetics of reversible protein denaturation. A study on aplysia myoglobin, Biophys. Chemist. 10 (1979) 119–127.
[82] H.M. Marques, A.Q. Munro, T. Munro, M. Wet, P.R. Vashi, Coordination of N-donor ligands by the monomeric ferric porphyrin *N*-acetylmicroperoxidase-8, Inorg. Chem. 38 (1999) 2312–2319.
[83] P.J. Marsh, J. Silver, M.C.R. Symons, F.A. Taiwo, Mössbauer and electron paramagnetic resonance studies on some new bis-(ligated) porphyrinatoiron(III) complexes with aliphatic amines. Models for cytochrome *b*, J. Chem. Soc. Dalton Trans. 11 (1996) 2361–2369.
[84] P. Basu, N.V. Shokhirev, J.H. Enemark, F.A. Walker, NMR studies of hindered ligand rotation, magnetic anisotropy, curie behavior, proton spin relaxation, and ligand exchange in some novel oxomolybdenum(V)/iron (III) porphyrinate complexes, J. Am. Chem. Soc. 117 (1995) 9042–9055.
[85] K.J. Lachance-Galang, P.E. Doan, M.J. Clarke, U. Rao, A. Yamano, B. Hoffman, EPR and NMR spectra as probes of spin-density distribution in heterocyclic ligands coordinated in *trans*-$[L(Im)(NH_3)_4Ru^{III}]$: implications for long-range electron transfer. Crystal structure of *trans*-$[(Im)_2(NH_3)_4Ru]Cl_3{\cdot}H_2O$, J. Am. Chem. Soc. 117 (1995) 3529–3538.
[86] H.A.S. Silva, R.M. Carlos, A.J. Camargo, C.M.C. Picchi, R.H.A. Santos, B.R. McGarvey, D.W. Franco, Study of the O–Ru–N bonding in *trans*-$[Ru(NH_3)_4SO_4)L]^+$ complexes (L = imidazole, histidine and substituted

pyridines): an X-ray, EPR, spectroscopic and theoretical MO study, Inorg. Chim. Acta 357 (2004) 3147–3154.
[87] H.A.S. Silva, B.R. McGarvey, R.H.D. Santos, M. Bertotti, V. Mori, D.W. Franco, Sulfate as a ligand in ruthenium(II) and (III) ammines, Can. J. Chem. 79 (2001) 679–687.
[88] D. Mohajer, G. Karimipour, M. Bagherzadeh, Reactivity studies of biomimetic catalytic epoxidation of alkenes with tetrabutylammonium periodate in the presence of various manganese porphyrins and nitrogen donors: significant axial ligand pi-bonding effects, New J. Chem. 28 (2004) 740–747.
[89] C.R. Johnson, C.M. Jones, S.A. Asher, J.E. Abola, Evaluation of the π-bonding ability of imidazole: structure determination and characterization of *catena*-$(H_2O)_2(1\text{-}CH_3im)_2Mg(\mu\text{-}CN)(CN)_4(1\text{-}CH_3im)Fe^{III}\cdot H_2O$ (1-$CH_3$im = 1-Methylimidazole)1, Inorg. Chem. 30 (1991) 2120–2129.
[90] N.M. Scott, R. Dorta, E.D. Stevens, A. Correa, L. Cavallo, S.P. Nolan, Interaction of a bulky N-heterocyclic carbene ligand with Rh(I) and Ir(I). Double C–H activation and isolation of bare 14-electron Rh(III) and Ir (III) complexes, J. Am. Chem. Soc. 127 (2005) 3516–3526.
[91] T.G. Spiro, J.M. Burke, Protein control of porphyrin conformation. Comparison of resonance Raman spectra of heme proteins with mesoporphyrin IX analogues, J. Am. Chem. Soc. 98 (1976) 5482–5489.
[92] F. Nastri, A. Lombardi, G. Morelli, C. Pedone, V. Pavone, G. Chottard, P. Battioni, D. Mansuy, Hemoprotein models based on a covalent helix-heme-helix sandwich: 3. Coordination properties, reactivity and catalytic application of Fe(III)- and Fe(II)-mimochrome I, J. Biol. Inorg. Chem. 3 (1998) 671–681.
[93] G. Ghirlanda, A. Osyczka, W. Lu, M. Antolovich, K.M. Smith, P.L. Dutton, A.J. Wand, W.F. DeGrado, *De Novo* design of a $D_2$-symmetrical protein that reproduces the diheme four-helix bundle in cytochrome $b_{c1}$, J. Am. Chem. Soc. 126 (2004) 8141–8147.
[94] A.P.S. Citadini, A.P.A. Pinto, A.P.U. Araújo, O.R. Nascimento, A.J. Costa-Filho, EPR studies of chlorocatechol 1,2-dioxygenase: evidences of iron reduction during catalysis and of the binding of amphipatic molecules, Biophys. J. 88 (2005) 3502–3508.
[95] S.V. Nistor, E. Goovaerts, S. Van Doorslaer, S. Dewilde, L. Moens, EPR-spectroscopic evidence of a dominant His-$Fe^{III}$-His coordination in ferric neuroglobin, Chem. Phys. Lett. 361 (2002) 355–361.
[96] F.A. Walker, Magnetic spectroscopic (EPR, ESEEM, Mössbauer, MCD and NMR) studies of low-spin ferriheme centers and their corresponding heme proteins, Coord. Chem. Rev. 185–186 (1999) 471–534.
[97] C.T. Migita, M. Iwaizumi, Low-temperature ePR studies of highly anisotropic low-spin (Protoporphyrinato)iron(III) complexes, J. Am. Chem. Soc. 103 (1981) 4378–4381.
[98] M. Fahnenschmidt, R. Bittl, H.K. Rau, W. Haehnel, W. Lubitz, Electron paramagnetic resonance and electron nuclear double resonance spectroscopy of a heme protein maquette, Chem. Phys. Lett. 323 (2000) 329–339.
[99] G. Gonzalez, E.M. Dioum, C.M. Bertolucci, T. Tomita, M. Ikeda-Saito, M.R. Cheesman, N.J. Watmough, M. Gilles-Gonzalez, Nature of the displaceable heme-axial residue in the *Ec*Dos protein, a heme-based sensor from *Escherichia coli*, Biochemistry 41 (2002) 8414–8421.
[100] J. Peterson, C. Vibat, R.B. Gennis, Identification of the axial heme ligands of cytochrome $b_{556}$ in succinate: ubiquinone oxidoreductase from *Escherichia coli*, FEBS Lett. 355 (1994) 155–156.
[101] M.P. Hendrich, A.K. Upadhyay, J. Riga, D.M. Arciero, A.B. Hooper, Spectroscopic characterization of the NO adduct of hydroxylamine oxidoreductase, Biochemistry 41 (2002) 4603–4611.
[102] L. Duclund, H. Toftlund, Electron paramagnetic resonance characteristics of some non-heme low-spin iron(III) complexes, Spectrochim. Acta, Part A 56 (2000) 331–340.
[103] D.M. Arciero, Q. Peng, J. Peterson, A.B. Hooper, Identification of axial ligands of cytochrome $c_{552}$ from *Nitrosomonas europaea*, FEBS Lett. 342 (1994) 217–220.
[104] S.D. Zaric, D.M. Popovic, E. Knapp, Factors determining the orientation of axially coordinated imidazoles in heme proteins, Biochemistry 40 (2001) 7914–7928.
[105] V. Medakovic, S.D. Zaric, Theoretical study on orientations of axially coordinated imidazoles in model systems of cytochromes, Inorg. Chim. Acta 349 (2003) 1–5.
[106] B.R. McGarvey, Survey of ligand field parameters of strong field $d^5$ complexes obtained from the *g* matrix, Coord. Chem. Rev. 170 (1998) 75–92.
[107] P.H. Rieger, Electron paramagnetic resonance studies of low-spin $d^5$ transition metal complexes, Coord. Chem. Rev. 135/136 (1994) 203–286.
[108] L.A. Yatsunyk, N.V. Shokhirev, F.A. Walker, Magnetic resonance spectroscopic investigations of the electronic ground and excited states in strongly nonplanar iron(III), Inorg. Chem. 44 (2005) 2848–2866.
[109] H. Ogura, L. Yatsunyk, C.J. Medforth, K.M. Smith, K.M. Barkigia, M.W. Renner, D. Melamed, F.A. Walker, Molecular structures and magnetic resonance spectroscopic investigations of highly distorted six-coordinate low-spin iron(III) porphyrinate complexes, J. Am. Chem. Soc. 123 (2001) 6564–6578.
[110] R. Benda, V. Schünemann, A.X. Trautwein, S. Cai, J.R. Polam, C.T. Watson, T.K. Shokhireva, F.A. Walker, Models of the bis-histidine-coordinated ferricytochromes: Mössbauer and EPR spectroscopic studies of low-spin iron(III) tetrapyrroles of various electronic ground states and axial ligand orientations, J. Biol. Inorg. Chem. 8 (2003) 787–801.
[111] F.A. Walker, B.H. Huynh, W.R. Scheidt, S.R. Osvath, Models of the cytochrome *b*. Effect of axial ligand plane orientation on the EPR and Mössbauer spectra of low-spin ferrihemes, J. Am. Chem. Soc. 108 (1986) 5288–5297.
[112] M.K. Safo, F.A. Walker, A.M. Raitsimring, W.P. Walters, D.P. Dolata, P.G. Debrunner, W.R. Scheidt, Axial ligand orientation in iron(III) porphyrinates: effect of axial π-acceptors. Characterization of the low-spin complex $[Fe(TPP)(4\text{-}CNPy)_2]ClO_4$, J. Am. Chem. Soc. 116 (1994) 7760–7770.
[113] M.J.M. Nesset, S. Cai, T.K. Shokhireva, N.V. Shokhirev, S.E. Jacobson, K. Jayaraj, A. Gold, F.A. Walker, Electronic effects in transition metal porphyrins. 10. Effect of *Ortho* substituents on the temperature dependence of the NMR spectra of a series of spin-admixed perchloratoiron(III) tetrakis(2,6- or 2,4,6-phenyl substituted)porphyrinates, Inorg. Chem. 39 (2000) 532–540.
[114] J.P. Simonato, J. Pecaut, L. Le Pape, J.L. Oddou, C. Jeandey, M. Shang, W.R. Scheidt, J. Wojaczynski, S. Wolowiec, L. Latos-Grazynski, J.C. Marchon, An integrated approach to the mid-spin state ($S$=3/2) in six-coordinate iron(III) chiroporphyrins, Inorg. Chem. 39 (2000) 3978–3987.
[115] L.A. Yatsunyk, M.D. Carducci, F.A. Walker, Low-spin ferriheme models of the cytochromes: correlation of molecular structure with EPR spectral type, J. Am. Chem. Soc. 125 (2003) 15986–16005.
[116] J.S. Griffith, Theory of E. P. R. in low-spin ferric haemoproteins, Mol. Phys. 21 (1971) 135–139.
[117] O. Iakovleva, M. Reiner, H. Rau, W. Hachnel, F. Parak, Mössbauer and EPR study of a cytochrome *b* model, Phys. Chem. Chem. Phys. 4 (2002) 655–660.
[118] M.K. Safo, G.P. Gupta, C.T. Watson, U. Simonis, F.A. Walker, W.R. Scheidt, Models of the cytochrome *b*. Low-spin bis-ligated (Porphinato) iron(III) complexes with "Unusual" molecular structures and NMR, EPR, and Mössbauer spectra, J. Am. Chem. Soc. 114 (1992) 7066–7075.
[119] J. Tsuka, One interpretation of the thermal equilibrium between high-spin and low-spin states in ferrihemproteins, Biochim. Biophys. Acta 214 (1970) 233–235.
[120] M.G. Mainwaring, S.D. Lugo, R.A. Fingal, O.H. Kapp, S.N. Vinogradov, The dissociation of the extracellular hemoglobin of *Lumbricus terrestris* at acid pH and its reassociation at neutral pH—a new model of its quaternary structure, J. Biol. Chem. 261 (1986) 10899–10908.
[121] M.H. Emptage, A.V. Xavier, J.M. Wood, B.M. Alsaadi, G.R. Moore, R.C. Pitt, R.J.P. Williams, R.P. Ampler, R.G. Bartsch, Nuclear magnetic resonance studies of *Rhodospirillum rubrum* cytochrome *c*′, Biochemistry 20 (1981) 58–64.
[122] C. Hundahl, A. Fago, R.E. Weber, Effects of water activity on oxygen-binding in high-molecular weight, extracellular invertebrate hemoglobin and hemocyanin, Comp. Biochem. Physiol. 136B (2003) 83–90.
[123] Y. Zeng, G.A. Caignan, R.A. Bunce, J.C. Rodriguez, A. Wilks, M. Rivera, Azide-inhibited bacterial heme oxygenases exhibit an $S$=3/2 $(d_{xz},d_{yz})^3(d_{xy})^1(d_z^2)^1$ spin state: mechanistic implications for heme oxidation, J. Am. Chem. Soc. 127 (2005) 9794–9807.

[124] Y. Mie, F. Mizutani, T. Uno, C. Yamada, K. Nishiyama, I. Taniguchi, Direct electrochemistry of engineered cytochrome $b_{562}$ molecules with a ligand binding pocket, J. Inorg. Biochem. 99 (2005) 1245–1249.
[125] S. Korenaga, J. Igarashi, A. Matsuoka, K. Shikama, A primitive myoglobin from *Tetrahymena pyriformis*: its heme environment, autoxidizability, and genomic DNA structure, Biochim. Biophys. Acta 1543 (2000) 131–145.
[126] M. Tsuruga, K. Shikama, Biphasic nature in the autoxidation reaction of human oxyhemoglobin, Biochim. Biophys. Acta 1337 (1997) 96–104.
[127] K. Shikama, A. Matsuoka, H. Iwaasa, The unique structures of protozoan myoglobin and yeast hemoglobin: an evolutionary diversity, Int. J. Biochem. Cell Biol. 27 (1995) 1107–1115.